

Efficient Surface Treatment to Improve Contact Properties of Inkjet-Printed Short-Channel Organic Thin-Film Transistors

Jewook Ha¹, Jiseok Seo¹, Seunghwan Lee¹, Eunho Oh¹, Takhee Lee²,
Seungjun Chung^{2,*}, and Yongtaek Hong^{1,*}

¹*Department of Electrical and Computer Engineering and Inter-University Semiconductor Research Center (ISRC), Seoul National University, Seoul 08826, Republic of Korea*

²*Department of Physics and Astronomy, Seoul National University, Seoul 08826, Republic of Korea*

In this paper, we report contact properties of fully inkjet-printed organic thin-film transistors (OTFTs) with various channel lengths and their improvement by introducing an organo-compatible interlayer between the organic channel and inkjet-printed metallic contacts. To realize all-inkjet-printed OTFTs, a highly conductive metal-organic precursor type silver ink, poly(4-vinylphenol), chlorosilane-terminated polystyrene (PS) and 6,13-bis(triisopropylsilylethynyl)pentacene (TIPS pentacene) solutions were printed by using a commercial piezoelectric inkjet-printer for gate and source/drain (*S/D*) electrodes, a gate dielectric layer, an interface engineering layer, and a semiconductor layer, respectively. Especially, since the contact resistance more dominantly affects a carrier injection property as channel length gets short, a short-channel length of 7 μm was formed by using 1 picoliter volume ink cartridge to investigate effects of the organo-compatible interlayer obviously. To evaluate contact properties of the inkjet-printed short-channel OTFTs, transmission line method and Y-function method analyses were used for various channel lengths and low drain-to-source voltage (V_{DS}) regime of -5 V, respectively. The contact properties between inkjet-printed silver *S/D* electrodes and TIPS pentacene semiconductor were drastically enhanced showing contact resistance lowered by an order of magnitude and a good linearity at low V_{DS} regime after inserting an end-functionalized PS layer.

Keywords: Organic Thin-Film Transistors, Inkjet Printing, Contact Resistance, Interface Engineering.

1. INTRODUCTION

Printed organic thin-film transistors (OTFTs) have been widely reported as emerging potential driving components for flexible and large-area electronic applications due to their ability to use low-temperature processing without vacuum processes.^{1–6} Among large-scale solution printing methods, a maskless drop-on-demand inkjet-printing process allows a low-cost fabrication without the waste of materials and contact-related contamination for realizing large-area electronics.^{4–6} However, owing to the poor organic solvent and thermal resistance of the printed organic semiconductors, bottom-contact structures have been typically adopted instead of top-contact ones.^{1,3–6}

Therefore, printing of organic semiconductors onto bottom source and drain (*S/D*) electrodes and gate dielectrics results in a high contact resistance as well as unfavorable crystal structures of π -conjugated semiconductors during drying of solvents near *S/D* electrodes, yielding poor electrical performance, even if the devices are fully dedicated and aligned, compared to vacuum-processed systems.^{7,8} Moreover, as demand for short-channel OTFTs has been significantly increased for improvement of on-state current and maximum operating frequency in highly integrated systems,^{9–11} contact properties between organic semiconductors and inorganic *S/D* electrodes should be addressed because contact resistance is one of the most critical factors for electrical characteristics of OTFTs by dominantly affecting a carrier injection property as the channel length gets short.^{12–14}

*Authors to whom correspondence should be addressed.

In this paper, we report enhanced contact properties of fully inkjet-printed short-channel OTFTs by introducing a chlorosilane-terminated polystyrene interlayer (PS-brush interlayer) between the S/D electrodes and semiconductor layers. The end-functionalized PS layer allows not only the better contact properties by introducing an organo-compatible interface on the contacts, but uniformly deposited printed organic semiconductor layers by providing a smooth and sufficiently hydrophobic surface.¹⁵ The contact properties were analyzed by using both transmission line method (TLM) and Y -function method (YFM).

2. EXPERIMENTAL DETAILS

Figure 1(a) illustrates procedure of fabricating all-inkjet-printed OTFTs with various channel lengths in order to examine the contact resistance between the S/D electrodes and organic semiconductor layer using TLM. Onto the cleaned substrate, a metal-organic precursor type silver ink (Jet-001T, Hisense Electronics Corp.) was inkjet-printed to form a gate electrode, and then sintered at 150 °C for 30 min. The width and height of the gate electrode were 610 μm and 200 nm, respectively. For a gate dielectric layer, a poly(4-vinylphenol) (PVP) solution composed of 10 wt.% of PVP powder and 2 wt.% of poly(melamine-*co*-formaldehyde) as a cross-linking agent dissolved in

propylene glycol methyl ether acetate was inkjet-printed in 2 passes. A ramped curing condition for the PVP dielectric layer was used to eliminate the formation of pin holes, and to allow a smoother surface.⁶ For short-channel length and narrow S/D electrodes formation, nozzles with a small diameter of 9 μm that can eject 1 pL volume of ink droplets were used. Note that 2-pass-printed S/D electrodes were used to deliver better conductivity and surface properties. To introduce an organo-compatible PS-brush interlayer, a 0.4 wt.% dimethylchlorosilane-terminated PS (PS-Si(CH₃)₂Cl, $M_n = 8$ kDa, Polymer Source Inc.) solution dissolved in toluene was also inkjet-printed onto both the S/D electrodes and channel region, followed by being annealed at 100 °C for 1 h to deliver a chemically-stable monolayer coupled with the hydroxyl groups (–OH) on the dielectric. After annealing, the non-coupled residue was rinsed with toluene. Finally, for the formation of semiconductor layer, a 1 wt.% 6,13-bis(triisopropylsilylethynyl)pentacene (TIPS pentacene) (EM-index Corp.) solution dissolved in toluene was inkjet-printed onto the channel and contact region, and then dried at room temperature in ambient air. All layers in the device were inkjet-printed using a piezoelectric inkjet printer (DMP-2831, Dimatix Corp.). All measurements were performed at room temperature in ambient air.

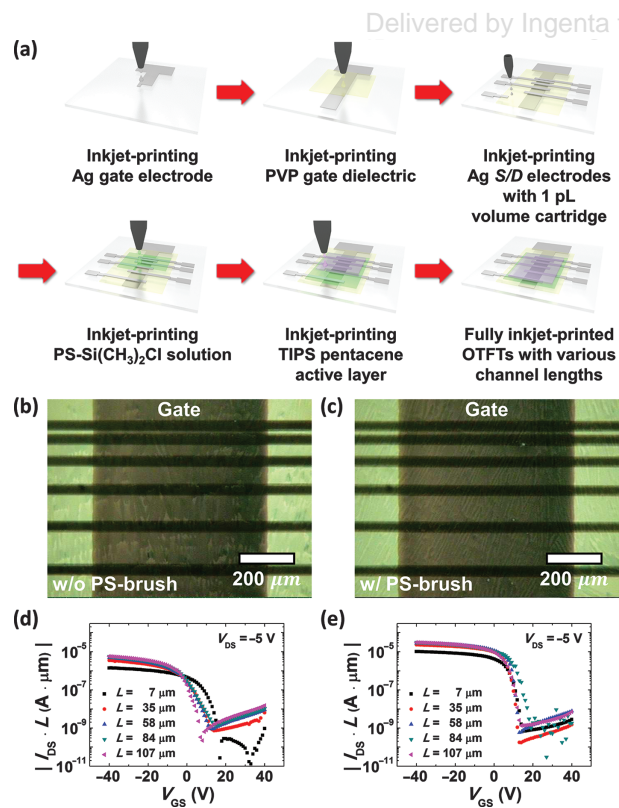


Figure 1. (a) Fabrication procedure of all-inkjet-printed OTFTs with various channel lengths. Optical images of the OTFTs (b) without and (c) with the PS-brush interlayer. Channel length normalized transfer curves of the OTFTs (d) without and (e) with a PS-brush interlayer.

3. RESULTS AND DISCUSSION

To achieve good contact properties between solution-processed organic semiconductor layers and inorganic contacts, surface energy matching between the gate dielectric layers and S/D electrodes should be guaranteed to form well-crystallized semiconductor layers near the channel-contact boundary. The chemically-coupled PS-brush layer allowed an organo-compatible surface on the inkjet-printed Ag electrodes providing a sufficient hydrophobic surface to produce highly ordered crystal structures of TIPS pentacene. Also, the interlayer delivered an excellent wetting property of TIPS pentacene semiconductor ink on both the gate dielectric layer and the S/D electrodes in a single-step, resulting in uniformly deposited π -conjugated semiconductor layers without discontinuous crystals (Figs. 1(b) and (c)). Figures 1(d) and (e) show the channel length normalized transfer curves of the OTFTs without and with the PS-brush interlayer, respectively. Because the contact resistance dominantly affects electrical performances of short-channel OTFTs, the length-normalized drain-to-source current (I_{DS}) was lowered as the channel length of the OTFTs shortened. This phenomenon also could be observed from the output characteristics of the OTFTs having a channel length of 7 μm (Figs. 2(a) and (b)) comparing with those of the OTFTs having a channel length of 107 μm (Figs. 2(c) and (d)). Although short-channel OTFTs still show more obvious S -shape at low drain-to-source voltage (V_{DS}) regime than those with a longer channel length, carrier injection properties of the OTFTs with the

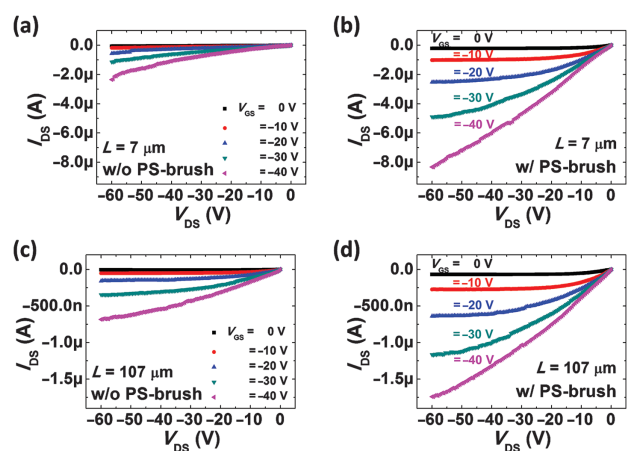


Figure 2. (a–b) Output curves of the OTFT having a channel length of 7 μm: (a) without (b) with the PS-brush interlayer. (c–d) Output curves of the OTFTs having a channel length of 107 μm: (c) without and (d) with the PS-brush interlayer.

PS-brush layer were drastically improved by enhancing the wetting and contact properties of TIPS pentacene near the contacts.

For further investigation of effects of the PS-brush interlayer to the inkjet-printed OTFTs, the contact resistances were extracted by employing two kinds of analyses: TLM and YFM. From the electrical characteristics of the OTFTs with various channel lengths, the contact resistances between the *S/D* electrodes and semiconductor layer were extracted using TLM. Because the on-state resistance (R_{on}) of the OTFTs is the sum of the channel resistance (R_{ch}) and the contact resistance (R_c), R_{on} can be expressed as following equation:^{16,17}

$$R_{on} = R_{ch} + R_c = \frac{1}{WC_{ins}\mu_{FE}(V_{GS} - V_{TH} - V_{DS}/2)}L + R_c \quad (1)$$

where L , W , C_{ins} , μ_{FE} , V_{GS} and V_{TH} denote a channel length, a channel width, capacitance per unit area of the gate insulator, a field-effect mobility, a gate-to-source voltage, and a threshold voltage, respectively. From the Eq. (1), R_c can be assumed as R_{on} when the channel length is equal to 0 because R_{ch} is proportional to the channel length. From the relationship of R_{on} and the channel length in Figures 3(a and b), the contact resistance of the OTFTs drastically reduced from 28.2 MΩ (=1.72 MΩ·cm) to 3.47 MΩ (=0.211 MΩ·cm) after introducing the PS-brush interlayer. The contact resistance of the OTFTs without the PS-brush interlayer is consistent with the previously reported result.^{8,18} Also, the logarithmic plot of the output characteristics as shown in Figure 3(c) supports enhanced carrier injection properties after introducing the PS-brush layer due to the lower contact resistance showing a better linearity at low V_{DS} regime.

The contact resistances were also extracted using YFM which is known as useful method to extract a mobility, a

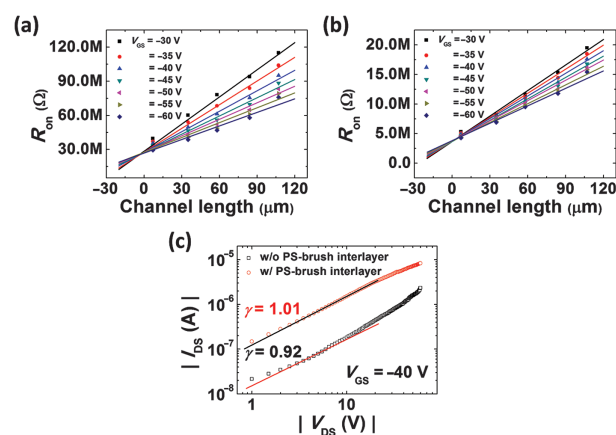


Figure 3. TLM results for the OTFTs (a) before and (b) after introducing the PS-brush interlayer. (c) The I_{DS} – V_{DS} relationship of short-channel OTFTs with and without the PS-brush interlayer in a logarithmic scale (γ value closed to 1 means a good linearity).

threshold voltage, and a contact resistance.^{19–22} Y -function can be expressed as following equation:

$$Y = \frac{I_{DS}}{\sqrt{g_m}} \quad (2)$$

where g_m denotes the transconductance. Assuming that V_{DS} is much smaller than $V_{GS} - V_{TH}$, I_{DS} can be approximated as:²²

$$I_{DS} \cong \mu_0 C_{ins} \frac{W}{L} (V_{GS} - V_{TH})(V_{DS} - I_{DS} R_c) \quad (3)$$

where μ_0 denotes a low field mobility. From the Eqs. (2) and (3), Y -function can be expressed as:

$$Y = \sqrt{\mu_0 C_{ins} V_{DS} \frac{W}{L} (V_{GS} - V_{TH})} \quad (4)$$

Therefore, from the Y -function– V_{GS} graph in Figures 4(a and b), μ_0 and V_{TH} can be extracted from the slope and the x -intercept, respectively.

After then, the contact resistance can be calculated from the following equation:

$$R_c = R_{on} - R_{ch} = \left| \frac{V_{DS}}{I_{DS}} \right| - \left| \frac{1}{\mu_0 C_{ins} (W/L) (V_{GS} - V_{TH})} \right| \quad (5)$$

Substituting μ_0 and V_{TH} to the acquired values from YFM, the contact resistances could be calculated. The

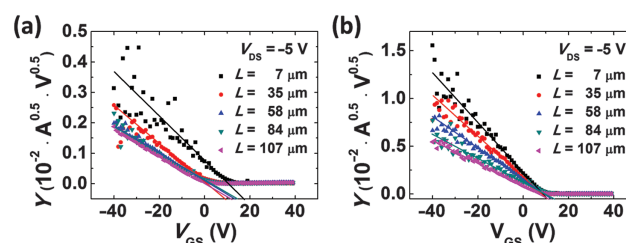


Figure 4. Y -function– V_{GS} graphs of the OTFTs with various channel lengths (a) without and (b) with the PS-brush interlayer.

Table I. Summary for electrical properties of the OTFTs without and with the PS-brush interlayer.

	μ_{FE} [$\text{cm}^2 \cdot \text{V}^{-1} \cdot \text{s}^{-1}$]	On/off ratio	R_c extracted by TLM [$\text{M}\Omega \cdot \text{cm}$]	R_c extracted by YFM [$\text{M}\Omega \cdot \text{cm}$]	N_{SS}^{max} [$\text{cm}^{-2} \cdot \text{eV}^{-1}$]
w/o PS-brush	0.00816	1.08×10^4	1.72	1.65	1.74×10^{12}
w/ PS-brush	0.125	3.73×10^4	0.211	0.277	6.93×10^{11}

contact resistances without and with the PS-brush interlayer were 27.1 $\text{M}\Omega$ ($=1.65 \text{ M}\Omega \cdot \text{cm}$) to 4.54 $\text{M}\Omega$ ($=0.277 \text{ M}\Omega \cdot \text{cm}$) which are consistent with the extracted contact resistances by TLM. Electrical characteristics of the short-channel OTFTs including the contact resistances extracted from both the TLM and YFM are summarized in Table I. From the extracted contact resistance values, it could be concluded that the PS-brush interlayer delivered improved contact properties between the metallic contacts and organic semiconductor layer resulting in one order of magnitude reduced contact resistance. The rate of this improvement is comparable with those of the previously reported results.^{23–25} Also, a facile printing method allowed a low-cost, easy and fast processing on large-area platforms.

4. CONCLUSION

In this paper, enhanced contact properties by conducting organo-compatible interface engineering between silver S/D electrodes and TIPS pentacene organic semiconductor layers for all-inkjet-printed OTFTs with a bottom-contact configuration were reported. The contact properties between the S/D electrodes and organic semiconductors were fully investigated by using both TLM at various carrier concentrations and YFM at various channel lengths, and the contact resistances extracted by two methods were well-agreed. By introducing the organo-compatible PS-brush interlayer, the contact resistance was reduced by an order of magnitude showing a better carrier injection property. Based on these results, we believe this interface engineering approach can be an attractive candidate to solve contact-related issues for realizing low-cost and highly integrated inkjet-printed short-channel OTFTs and their applications.

Acknowledgment: J. Ha and Y. Hong appreciate the support from the Center for Advanced Soft-Electronics funded by the Ministry of Science, ICT and Future Planning as Global Frontier Project (CASE-2015M3A6A5065309). S. Chung and T. Lee appreciate the support from the National Creative Research Laboratory program (Grant No. 2012026372) funded by the Korean Ministry of Science, ICT and Future Planning.

References and Notes

- J. Jo, J.-S. Yu, T.-M. Lee, and D.-S. Kim, *Jpn. J. Appl. Phys.* 48, 04C181 (2009).
- B. Peng, X. Ren, Z. Wang, X. Wang, R. C. Roberts, and P. K. L. Chan, *Sci. Rep.* 4, 6430 (2014).
- M. Vilkmann, T. Hassinen, M. Keränen, R. Pretot, P. van der Schaaf, T. Ruotsalainen, and H. G. O. Sandberg, *Org. Electron.* 20, 8 (2015).
- K. Fukuda, Y. Takeda, Y. Yoshimura, R. Shiwaku, L. T. Tran, T. Sekine, M. Mizukami, D. Kumaki, and S. Tokito, *Nat. Commun.* 5, 4147 (2014).
- D. Kim, S. H. Lee, S. Jeong, and J. Moon, *Electrochem. Solid-State Lett.* 12, H195 (2009).
- S. Chung, S. O. Kim, S.-K. Kwon, C. Lee, and Y. Hong, *IEEE Electron Device Lett.* 32, 1134 (2011).
- X. Li, W. T. T. Smaal, C. Kjellander, B. van der Putten, K. Gualandris, E. C. P. Smits, J. Anthony, D. J. Broer, P. W. M. Blom, J. Genoe, and G. Gelinck, *Org. Electron.* 12, 1319 (2011).
- S. Chung, J. Jeong, D. Kim, Y. Park, C. Lee, and Y. Hong, *J. Display Technol.* 8, 48 (2012).
- H.-Y. Tseng, B. Purushothaman, J. Anthony, and V. Subramanian, *Org. Electron.* 12, 1120 (2011).
- J. Jeon, B. C.-K. Tee, B. Murmann, and Z. Bao, *Appl. Phys. Lett.* 100, 043301 (2012).
- A. Reuveny, T. Yokota, R. Shidachi, T. Sekitani, and T. Someya, *Org. Electron.* 26, 279 (2015).
- L. Torsi, A. Dodabalapur, and H. E. Katz, *J. Appl. Phys.* 78, 1088 (1995).
- G. S. Tulevski, C. Nuckolls, A. Afzali, T. O. Graham, and C. R. Kagan, *Appl. Phys. Lett.* 89, 183101 (2006).
- B. Stadlober, U. Haas, H. Gold, A. Haase, G. Jakopic, G. Leising, N. Koch, S. Rentenberger, and E. Zojer, *Adv. Funct. Mater.* 17, 2687 (2007).
- S. Chung, M. Jang, S.-B. Ji, H. Im, N. Seong, J. Ha, S.-K. Kwon, Y.-H. Kim, H. Yang, and Y. Hong, *Adv. Mater.* 25, 4773 (2013).
- P. V. Necliudov, M. S. Shur, D. J. Gundlach, and T. N. Jackson, *Solid-State Electron.* 47, 259 (2003).
- G. B. Blanchet, C. R. Fincher, M. Lefenfeld, and J. A. Rogers, *Appl. Phys. Lett.* 84, 296 (2004).
- P. V. Pesavento, K. P. Puntambekar, C. D. Frisbie, J. C. McKeen, and P. P. Ruden, *J. Appl. Phys.* 99, 094504 (2006).
- G. Ghibaudo, *Electron. Lett.* 24, 543 (1988).
- Y. Xu, T. Minari, K. Tsukagoshi, J. A. Chroboczek, and G. Ghibaudo, *J. Appl. Phys.* 107, 114507 (2010).
- O. Marinov, M. J. Deen, C. Feng, and Y. Wu, *J. Appl. Phys.* 115, 034506 (2014).
- H.-Y. Chang, W. Zhu, and D. Akinwande, *Appl. Phys. Lett.* 104, 113504 (2014).
- D. Boudinet, G. L. Blevenec, C. Serbutoviez, J.-M. Verilhac, H. Yan, and G. Horowitz, *J. Appl. Phys.* 105, 084510 (2009).
- Y. Xie, S. Cai, Q. Shi, S. Ouyang, W.-Y. Lee, Z. Bao, J. R. Matthews, R. A. Bellman, M. He, and H. H. Fong, *Org. Electron.* 15, 2073 (2014).
- J. Lee, J. S. Park, B.-L. Lee, J.-I. Park, J. W. Chung, and S. Lee, *Org. Electron.* 15, 2021 (2014).

Received: 3 June 2016. Accepted: 30 August 2016.